TAZ Promotes PC2 Degradation through a SCF$^{\beta\text{-Trcp}}$ E3 Ligase Complex[∇][†]

Yu Tian,[1] Robert Kolb,[2] Jeong-Ho Hong,[3,4] John Carroll,[1] Dawei Li,[1] John You,[1] Roderick Bronson,[1] Michael B. Yaffe,[3] Jing Zhou,[2] and Thomas Benjamin[1]*

Department of Pathology[1] and Brigham and Women's Hospital,[2] Harvard Medical School, Boston, Massachusetts 02115; Center for Cancer Research, Massachusetts Institute of Technology, Cambridge, Massachusetts 02139[3]; and School of Life Sciences and Biotechnology, Korea University, Anam-Dong, Seongbuk-Gu, Seoul 136-701, South Korea[4]

Studies of a TAZ knockout mouse reveal a novel function of the transcriptional regulator TAZ, that is, as a binding partner of the F-box protein β-Trcp. TAZ$^{-/-}$ mice develop polycystic kidney disease (PKD) and emphysema. The calcium-permeable cation channel protein polycystin 2 (PC2) is overexpressed in kidneys of TAZ$^{-/-}$ mice as a result of decreased degradation via an SCF$^{\beta\text{-Trcp}}$ E3 ubiquitin ligase pathway. Replacements of serines in a phosphodegron motif in TAZ prevent β-Trcp binding and PC2 degradation. Coexpression of a cytoplasmic fragment of polycystin 1 blocks the PC2-TAZ interaction and prevents TAZ-mediated degradation of PC2. Depletion of TAZ in zebrafish also results in a cystic kidney accompanied by overexpression of PC2. These results establish a common role of TAZ across vertebrate species in a protein degradation pathway regulated by phosphorylation and implicate deficiencies in this pathway in the development of PKD.

First reported as a 14-3-3 binding protein, TAZ (*transcriptional coactivator with PDZ binding motif*) (29) exhibits transcriptional regulatory functions in conjunction with a variety of transcription factors. These include members of the RUNX family (1, 9, 29, 34, 35), T-box transcription factor TBX5 (40), Pax3 (paired box homeotic gene 3) (41), TEF-1 (transcriptional enhancer factor 1) (37), and TTF-1 (thyroid transcription factor 1) (45) and peroxisome proliferator receptor gamma (21). Nuclear localization and coactivator functions of TAZ are regulated in part through phosphorylation and 14-3-3 binding (29). TAZ regulates gene expression underlying aspects of development of bone (9, 21), muscle (37), fat (21), lung (45), and heart and limb (40). In mesenchymal stem cells TAZ functions as a modulator of transcription to facilitate and inhibit differentiation into osteoblast and adipocyte lineages, respectively (21). Together, these observations suggested that TAZ-deficient mice might show profound defects in the development of one or more of these mesenchyme-derived tissues.

Independently, TAZ was discovered as a binding target of the oncogenic mouse polyomavirus T (tumor) antigens (59). TAZ overexpression has an inhibitory effect on viral DNA replication. This inhibition is dependent in part on retention in the viral enhancer of the binding site for RUNX1/AML1, first described as the polyomavirus enhancer binding protein PEBP2α (27, 55). Infection by wild-type polyomavirus inhibits the transactivation function of TAZ. A polyomavirus mutant unable to bind TAZ is unable to transform cells and also unable to replicate and induce tumors in the mouse (unpublished observations). TAZ binds most strongly to the small and middle T antigens. These viral proteins function through complex formation with protein kinases and protein phosphatase

PP2A in the plasma membrane and cytosol. The effects of these two T antigens on TAZ are not readily explained in terms of transcriptional regulatory functions of TAZ. Rather, they suggest the possibility that TAZ possesses an additional phosphorylation-dependent function(s) distinct from its role in transcription.

To investigate TAZ functions in the context of a whole animal model, we have generated a TAZ knockout mouse. The pathological abnormalities in the surviving animals reveal new and unexpected molecular and physiological functions of TAZ as a component of an E3 ubiquitin ligase involved in ubiquitin-dependent substrate proteolysis. Surviving TAZ$^{-/-}$ mice develop two severe abnormalities: polycystic kidney disease and emphysema. In humans, autosomal dominant polycystic kidney disease (ADPKD) is due primarily to mutations in PKD1 and PKD2 encoding the transmembrane proteins polycystin 1 (PC1) and PC2, respectively (23, 26, 38, 66). The polycystins function together in mechanosensory transduction, coupled in some manner to primary cilia in renal epithelial cells and mediating an influx of extracellular calcium in response to fluid flow (42, 43, 47, 67). PC2 is a nonselective calcium-permeable cation channel protein (17, 20, 31, 36, 62). It is expressed in a broad range of tissues and mediates calcium entry (17, 36, 62) and calcium release from the endoplasmic reticulum following the initial influx of calcium (31, 32, 36). PC2 also plays a role along with PC1 in regulating cell growth via a JAK/STAT pathway and induction of p21^{waf1} (4). Here we show that in both mice and zebrafish, TAZ deficiency results in development of cysts in the kidney accompanied by accumulation of higher than normal levels of PC2. We show that phosphorylation of TAZ mediates its interaction with the F-box protein β-Trcp, forming part of an SCF$^{\beta\text{-Trcp}}$ E3 ligase complex that targets PC2 for degradation.

Note: while the manuscript was in preparation, a report was published on a knockout of Wwtrt1/TAZ in the mouse (22). This mouse develops glomerulocystic disease with little evidence of skeletal abnormalities. Results of the present study confirm these basic findings, though with some important dif-

ferences in severity and manifestations of disease. We also identify a new molecular function of TAZ and discuss its possible relevance to PKD.

MATERIALS AND METHODS

Generation of TAZ-null mice. The TAZ targeting vector was created by cloning 5.9-kb and 1.7-kb flanking genomic fragments of exon 2 into a pSAβ-galPGKneoPGKDTA vector (kindly provided by Haihua Gu, Beth Israel Hospital, Harvard Medical School). This vector encodes LacZ and contains a positive selection neomycin resistance cassette and a diphtheria toxin A chain expression negative selection cassette. The TAZ targeting vector was linearized and electroporated into embryonic stem (ES) cells. Resulting clones were screened for correct homologous recombination by PCR and Southern blot analysis. ES clones with a targeted disruption of the TAZ locus were injected into C57BL/6 blastocysts to produce chimeric mice; this was carried out in the Brigham and Women's Hospital Transgenic Mouse Facility. Chimeric mice were bred to 129S6 (aconic) mice to obtain germ line transmission. Subsequent breeding was carried out on a 126S6/SvEv background. The knockout was maintained by crossing animals heterozygous for the knockout allele.

Depletion of endogenous TAZ in zebrafish. Antisense morpholino oligonucleotides directed against the zebrafish translation initiation codon (zTAZ MO, 5′-CTGGAGAGGATTACCGCTCATGGTC-3′) and a standard control oligomer (control MO) were purchased from GeneTools LLC (Philomath, OR). Zebrafish embryos in the one- to two-cell stage were injected with 1 ng of oligonucleotides in 1× Danieua buffer (58 mM NaCl, 0.7 mM KCl, 0.4 mM MgSO₄, 0.6 mM CaNO₃ 2.5 mM HEPES, pH 7.6) and maintained as described previously (2). Eight days postfertilization, embryos were fixed, sectioned, and stained with hematoxylin and eosin (H&E). Three-day embryos were also examined by immunostaining using a rabbit anti-mouse PC2 antibody (see Fig. S3 in the supplemental material).

Histological analysis. Tissues were fixed in Bouin's solution, embedded in paraffin, sectioned at 5 μm, and stained with hematoxylin and eosin.

Plasmids and antibodies. A region of mPKD1 encoding a C-terminal cytoplasmic fragment of PC1 (amino acids 4066 to 4293), a region of mPKD2 encoding cytoplasmic fragment of PC2 (amino acids 678 to 966), and full-length mPKD2 cDNAs were amplified from a 17-day mouse embryo cDNA library (Clontech) and inserted into either N-terminal hemagglutinin (HA)-tagged eukaryotic expression vector pEBB, pcDNA3.1(+), or mammalian glutathione S-transferase (GST) fusion vector pEBG. TAZ constructs have been described elsewhere (59). PKD2 and TAZ mutant cDNA constructs were generated with the QuikChange site-directed mutagenesis kit (Stratagene) based on wild-type plasmids. Dominant-negative versions of hCul1 and hTrcp constructs, Trcp small interfering RNA (siRNA) construct Sh-Trcp, and control vector Sh-hrGFP and myc-tagged mTrcp1 and -2 constructs were kindly provided by Wade Harper, Department of Pathology, Harvard Medical School, and have been described previously (28).

Rabbit polyclonal anti-PC2 antibody (anti-PC2 5459) was generated using a bacterially expressed GST-PC2 C-terminal cytoplasmic fragment as antigen. Rabbit polyclonal anti-TAZ antibody has been described elsewhere (59). The following antibodies were also used: anti-PC1 (sc-10374 and sc-25570; Santa Cruz), anti-PC2 96525 (36), anti-HA (sc-7392 and sc-805; Santa Cruz), anti-β-tubulin (T0198; Sigma), anti-acetylated α-tubulin (T-6793; Sigma), anti-green fluorescent protein (anti-GFP; sc-8334; Santa Cruz), antiubiquitin (sc-8017; Santa Cruz), anti-Myc (sc-40; Santa Cruz), anti-Cul1 (71-8700; Zymed), anti-β-Trcp (37-3400; Zymed), anti-β-Trcp/HOS (sc-15354; Santa Cruz), anti-Kip1/p27 (K25020; Transduction Lab), anti-cdc-25A (MS-640-P0; NeoMarkers), c-Myc antibody-conjugated agarose (sc-789 AC; Santa Cruz), and c-Myc blocking peptide (sc-789P; Santa Cruz).

Immunohistochemistry and lectin staining. For immunohistochemistry, 5-μm sections were cut from the paraffin blocks, dewaxed, and serially rehydrated in water. Tissue sections were heated (98°C) and processed for epitope retrieval by incubation in sodium citrate buffer (10 mM sodium citrate, 0.05% Tween 20, pH 6.0), followed by a 20-min cool-down and treatment with 3% hydrogen peroxide before antibody application. Antibodies against PC1 (sc-10374; Santa Cruz) and PC2 (5459) were used. The avidin-biotin-peroxidase complex system (Vector Laboratories) was used to visualize immunohistochemical reactions along with Mayer's hematoxylin counterstain. Some sections were stained with tetramethyl rhodamine isothiocyanate-coupled *Dolichos biflorus* agglutinin or fluorescein isothiocyanate-coupled *Lotus tetragonolobus* agglutinin (Vector Laboratories).

Immunofluorescence. Baby mouse kidney (BMK) cells were plated in complete Dulbecco's modified Eagle's medium (DMEM) on coverslips and incu-

bated at 37°C. Cells were fixed with 4% paraformaldehyde in phosphate-buffered saline for 30 minutes and stained with rabbit polyclonal anti-TAZ, PC2 (5459), and mouse monoclonal anti-acetylated α-tubulin antibodies. The primary antibodies were detected with secondary Organ Green-conjugated anti-rabbit immunoglobulin G (IgG) antibody and rhodamine red-conjugated anti-mouse IgG antibody, respectively. IMCD cells were plated in DMEM–F-12 medium on coverslips and incubated at 37°C. After reaching 100% confluence, HA-tagged mTAZ was introduced into cells by transfection. Immunofluorescence was performed 24 h posttransfection using rabbit anti-HA polyclonal antibody (sc-805; Santa Cruz) for TAZ detection.

Real-time PCR. Total RNA was isolated from mouse kidney tissues using TRIzol reagent (Invitrogen), and oligo(dT)-based reverse transcription reactions were performed using SuperScript III (Invitrogen). The transcriptional levels of PKD1 and PKD2 genes in mouse kidneys and TAZ in human kidneys and cysts were checked by real-time PCR (SYBR Green, Lightcycler; Roche). Actin and glyceraldehyde-3-phosphate dehydrogenase (GAPDH) were used as internal controls. The following were primer sequences: mPKD1A206, GCCTCCATGCTGTGTTTGAAAGTC; mPKD1A654, GGACAGGTAAGGAAGGCAGCAATA; mPKD2A373, CGCCA TGTTTCCCTGATTCTGATG; mPKD2A758, ACTACCAGGAAGGTGACTA GGGAT mActin5, GTGGGCCGCTCATGGCACCAA; mActin3, CTCTTTGAT GTCACGCACGATTTC; GAPDHF, GCTGAACGGGAAGCTCACTGGCTA TGG; GAPDHR, GAGGCTCACCACCCTGTTGCTGTAGC. Three mice for each genotype and age group were used, and the reverse transcription-PCR experiments were carried out in triplicate.

Cell culture and transfection. 293 and BMK cells were cultured in DMEM supplemented with 10% heat-inactivated newborn calf serum and 100 U/ml penicillin and streptomycin. IMCD (ATCC CRL-2123) and established control and HA-mPC2-overexpressing IMCD cell lines were cultured in DMEM–F-12 medium with 10% fetal bovine serum. BMK cells were made from 10- to 14-day-old baby mice (63). 293 and IMCD cells were transfected with various expression plasmids and shRNA constructs for Trcp knock down by using Lipofectamine2000 (Invitrogen) per the manufacturer's instructions.

Retrovirus generation and infection. The pMXs-puro/Plat-E system was used to generate control and TAZ retroviruses (39) for infection of TAZ⁻/⁻ mouse embryonic fibroblasts.

Western blot analysis. Proteins were resolved by sodium dodecyl sulfate-polyacrylamide gel electrophoresis (SDS-PAGE) and transferred to a nitrocellulose membrane. The membranes were blocked with 5% nonfat milk–TNET buffer (10 mM Tris, 2.5 mM EDTA, 50 mM NaCl, and 0.1% Tween 20) for 1 h and probed with primary antibodies for 2 h at room temperature. After washing with TNE, the membranes were incubated with suitable secondary antibodies. Signals were detected with the Odyssey LI-COR infrared imaging system. PC2 levels in extracts of whole kidneys or cultured kidney epithelial cells were normalized to β-tubulin as an internal loading control.

Labeling cellular proteins with [³⁵S]methionine. Transfected 293 cells at 75% confluence were washed twice in DMEM without methionine and incubated for 6 h in methionine-deficient medium containing 2% calf serum and 50 μCi/ml [³⁵S]methionine. Cells were then washed and incubated further for different times in DMEM.

Immunoprecipitation and GST pull-down assay. For immunoprecipitations, cells were washed with phosphate-buffered saline and solubilized in NP-40 lysis buffer (20 mM Tris, pH 8.0, 135 mM NaCl, 1 mM MgCl₂, 0.1 mM CaCl₂, 10% glycerol, 1% NP-40, 0.1 mM Na₃VO₄, 50 mM β-glycerophosphate, 10 mM NaF, and the protease inhibitor Complete Mini from Roche). The lysates were incubated with the antibodies indicated and protein A–CL-4B (Amersham Pharmacia) for 2 h at 4°C. The beads were then washed five times with NP-40 lysis buffer, and the proteins were eluted by boiling in SDS-PAGE sampling buffer. For the GST pull-down assay, lysates of transfected cells were prepared with NP-40 lysis buffer 36 h posttransfection. Extracts (2 to 3 mg of protein) were incubated with glutathione-Sepharose 4B (Amersham Bioscience) at 4°C overnight, and the beads were washed with lysis buffer five times. The complexes were resolved on SDS-PAGE, and Western blotting was performed as described above.

Quantitation and statistical analysis. Bands from Western blots and autoradiography were quantified by Scion Image software. The standard *t* test was used to assess the significance of differences between means in PC2 levels of triplicate samples at each time point under different conditions of TAZ expression. A *P* value of <0.05 (one tail) was considered significant. The experiments on PC2 decay in Fig. 4A and 7E, below, were each repeated three times.

In vitro ubiquitylation. For PC2 in vitro ubiquitination, 1 μl of rabbit reticulocyte lysate-translated ³⁵S-labeled substrate PC2 was incubated in the absence or in the presence of increasing amounts of purified GST-TAZ and SCF^β-Trcp E3 ligase complex from transfected 293 cells, E1 ubiquitin-activating enzyme (50 ng), Ubc5 (200 ng), and ubiquitin (1 mg/ml) in a total volume of 20 μl. In
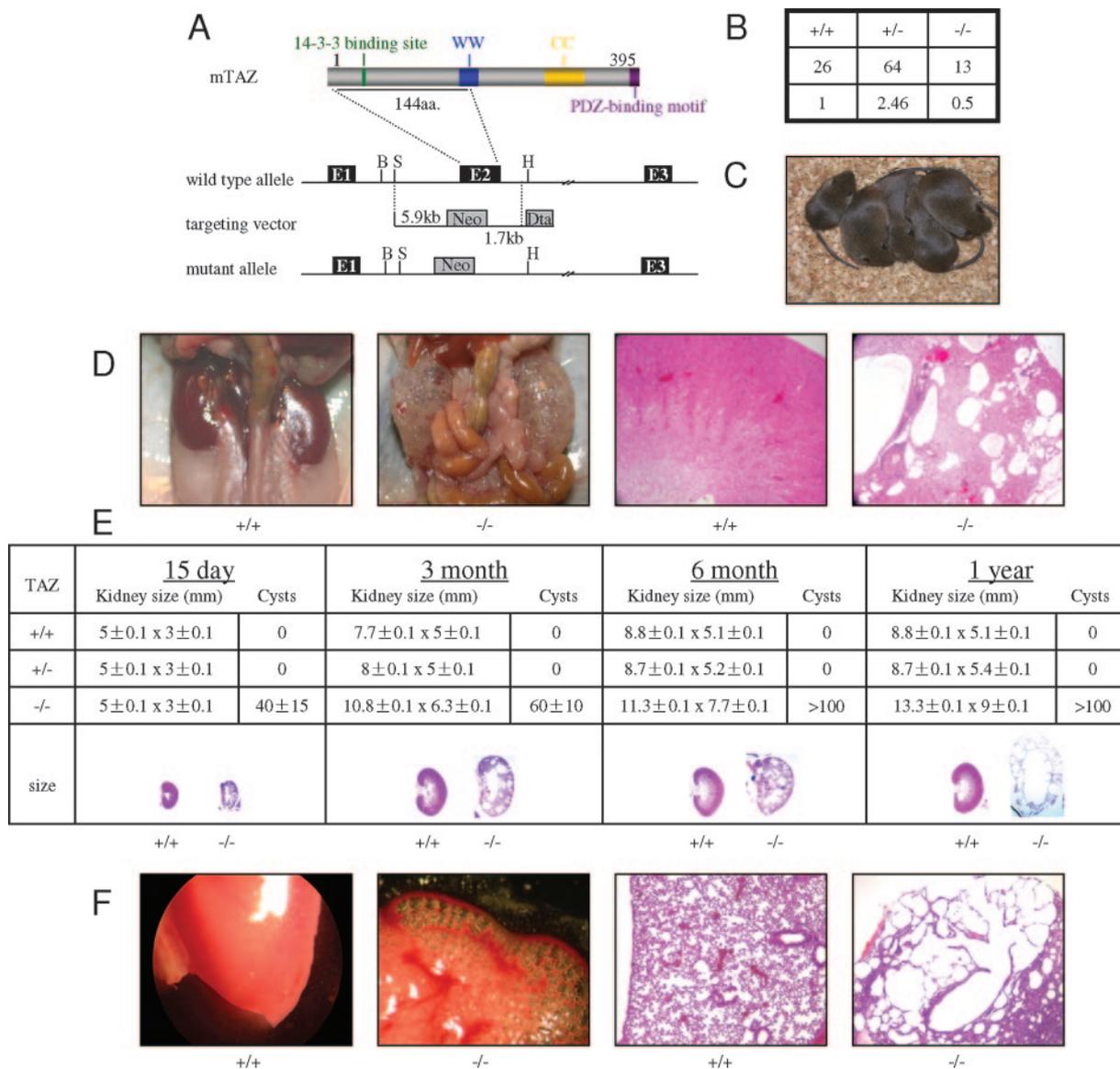
FIG. 1. TAZ$^{-/-}$ mice develop PKD and emphysema. (A) Generation of TAZ knockout mice. WW, WW domain; CC, coiled-coil region; E1, E2, and E3, exons 1, 2, and 3. Selective markers pGKneo and pGKtk are shown in shaded boxes. B, BglII; S, SacII; H, HindIII. (See Fig. S1 in the supplemental material for more detail.) (B) Progeny of +/− × +/− crosses. TAZ$^{-/-}$ mice were born at a lower-than-expected frequency. (C) Littermates from a heterozygous cross: the mouse on the left is −/−, and those on the right are either +/+ or +/−. (D) Gross and microscopic pictures of kidneys of normal (+/+) and affected (−/−) mice (139 days). Kidneys of the TAZ$^{-/-}$ mouse are enlarged with fluid-filled cysts. (E) Relative kidney size and number of cysts in TAZ$^{-/-}$ mice of different ages. (F) Gross and microscopic pictures of lungs of normal (+/+) and affected (−/−) mice (16 days). Lungs of the TAZ$^{-/-}$ mouse show swollen alveoli with breakdown of alveolar walls.

addition, reaction mixtures contained 25 mM Tris-HCl (pH 7.5), 60 mM NaCl, 1 mM dithiothreitol, 2 mM ATP, and 4 mM MgCl$_2$. After incubation at 30°C for 1.5 h, total reaction mixtures were electrophoresed in 4 to 14% SDS-PAGE gels, and the ^{35}S-labeled substrates were detected by autoradiography. Western blot assays for TAZ and Cul1 were also performed. Ubiquitin-activating enzyme E1 (E-305), conjugating enzyme E2 (UbcH5a, E2-616; UbcH3, E2-610), ubiquitin (U-100H), and energy regeneration solution (ERS; B-10) were all obtained from Boston Biochem.

RESULTS

A TAZ knockout mouse develops polycystic kidney disease and emphysema. A positive-negative selection vector (PGK-beta-galPGKneo; a gift from Haihua Gu) was used to replace exon 2 of TAZ in embryonic stem cells from 129SVE mice based on homologous recombination in flanking sequences. The targeting vector cassette is shown in Fig. 1A. Exon 2 of mouse TAZ encodes the first 144 amino acids of the protein; sequences downstream of the inserted vector are predicted to be out of frame. PCR and Southern blot analysis of the ES cell clone used to generate the knockout mouse showed a single insertion of the cassette at the expected site (see Fig. S1 in the supplemental material). No immunoreactive protein was detected by Western blotting using a polyclonal antiserum raised against a C-terminal fragment of mTAZ in tissues of knockout mice (see further below). Chimeric mice were crossed with

129S6 mice to identify offspring giving germ line transmission of the knockout allele. A single founder was used to establish a line of TAZ$^{-/-}$ mice, which has been maintained through crosses of heterozygous animals.

Loss of TAZ results in partial embryonic lethality. Crosses of TAZ$^{+/-}$ mice produced a dearth of $-/-$ pups which represented only half the expected number of offspring (Fig. 1B). Affected ($-/-$) mice were readily identified by their smaller size and relative inactivity compared to their normal littermates (Fig. 1C). These crosses produced heterozygous offspring at the expected frequency, and these mice were phenotypically normal.

Comprehensive histological examinations of $-/-$ mice were carried out at ages ranging from late gestation to 1 year. TAZ has been shown to function in mesenchymal stem cells as a transcriptional regulator, acting in conjunction with Runx2 to promote differentiation into osteoblasts and with peroxisome proliferator receptor gamma to inhibit differentiation into adipocytes (21). In addition, TAZ has known roles in transcriptional regulation of genes involved in cardiac and skeletal muscle differentiation and pulmonary surfactant production (37, 40, 45). Results carried out in part using embryonic fibroblasts from the TAZ knockout mouse (21) suggest that TAZ-deficient mice might manifest defects in development of bone and/or fat. However, TAZ$^{-/-}$ animals that survived, though runted, made bone and fat that were histologically normal. Adipocytes were somewhat diminished in size in $-/-$ compared to $+/+$ littermates, but no other differences were noted (see Fig. S2 in the supplemental material). While a defect(s) in mesenchymal cell differentiation may contribute to embryonic lethality, it does not appear to be manifested as abnormal development of either bone or fat in surviving mice.

We focused our attention on characterizing the surviving TAZ$^{-/-}$ animals and have not yet examined the mechanism of embryonic lethality. Surprisingly, the most profound abnormalities that were noted in the surviving TAZ$^{-/-}$ mice were the development of severe polycystic renal and pulmonary disease. Sections of kidneys of mutant mice from a few weeks of age up to 1 year showed changes typical of polycystic kidney disease with the development of round cysts of various sizes scattered throughout the cortex (Fig. 1D and E). Cysts were found bilaterally in every TAZ$^{-/-}$ animal, the earliest ones being seen in an 18-day TAZ$^{-/-}$ embryo. Cysts were uniformly lined by cuboidal epithelium with scanty cytoplasm. They frequently contained homogenous eosinophilic fluid or small amounts of floccular material. The renal pelvis was often moderately dilated in kidneys of younger $-/-$ mice. The number of cysts and overall kidney size were found to increase with age, akin to findings in human ADPKD (Fig. 1E).

TAZ$^{-/-}$ animals also developed emphysema, with swollen alveoli and breakdown of alveolar walls (Fig. 1F). More than 30 surviving TAZ$^{-/-}$ mice were examined, and all showed concomitant development of PKD and emphysema. Examination of tissues in several dozen mutant mice showed no cystic changes in salivary glands, pancreas, liver, or other glandular organs. Some 2- to 4-week-old mice were observed to have inflammation in lungs or intestines, presumably secondary to emphysema and renal disease. The major manifestations of TAZ deficiency, at least in the 129S6 background, appeared to be restricted to kidney and lung.

PC2 is overexpressed in kidneys of TAZ$^{-/-}$ mice. Kidney sections were first stained with fluorescent lectins to determine the segment of the nephron from which cysts arise in TAZ$^{-/-}$ mice (Fig. 2A). Cysts are found predominantly in the cortex, and these show positive staining with the lectin *Lotus tetragonolobus* agglutinin, indicating some cysts develop in proximal tubules, one of the segments affected in ADPKD (56). No staining was seen using the DBA lectin (*Dolichos biflorus* agglutinin), a marker for collecting ducts altered in the autosomal recessive form of the disease (68). Mutations in the polycystin genes PKD1 and PKD2 account for roughly 85% and 15% of human ADPKD, respectively (30, 49). PC1 and PC2 expression levels were therefore examined and compared in kidneys from age-matched $+/+$, $+/-$, and $-/-$ mice by immunostaining and Western blotting. Uniform weak tubular expression of PC1 was observed in kidney sections from both 3-month-old wild-type and mutant mice. No obvious differences in the level or distribution of PC1 staining were observed in kidneys from TAZ$^{-/-}$ mice based on immunostaining (Fig. 2B, upper panels) and Western blotting (Fig. 2C).

In contrast, expression of PC2 was clearly elevated in TAZ$^{-/-}$ mice. This was first shown using a previously characterized antiserum to an N-terminal peptide of mPC2 (anti-PC2 96525) (36). To confirm the initial findings, a new rabbit antiserum was raised against the C-terminal domain of mouse PC2 (anti-PC2 5459). Western blotting and immunoprecipitation experiments showed the same reactivity of the two antisera tested on transfected epitope-tagged PC2 and on the endogenous protein (see Fig. S3 in the supplemental material). In situ staining and Western blotting (Fig. 2C) of kidney extracts from wild-type and mutant mice were carried out with anti-PC2 5459. Tubules in mutant mice showed deep cytoplasmic staining concentrated mainly under the apical surfaces. Dense staining was seen in apparently normal ducts as well as in cells lining the cysts (Fig. 2B, middle panels). Tubules from wild-type controls showed a similar distribution but with considerably less intense staining compared to the mutant (Fig. 2B, compare lower panels). Overexpression of PC2 was also evident in the kidney of a TAZ$^{-/-}$ embryo of 14 to 15 days gestation without obvious development of cysts (Fig. 2B, lower panels).

PC2 overexpression was confirmed by Western blotting using extracts of kidneys from $+/+$, $+/-$, and $-/-$ mice sampled at different ages (Fig. 2C). Levels of PC2 in these extracts were quantitated based on the Western blot assays and normalized to β-tubulin by densitometry. β-Tubulin was used as a loading control because its levels in cultured mouse kidney cells were found to be unaffected by TAZ depletion (Fig. 2D). Levels of PC2 were consistently elevated 2- to 2.2-fold in $-/-$ compared to $+/+$ kidney tissue. PC2 levels were approximately the same in $+/+$ and $+/-$ animals, consistent with the normal gross and histological findings in these animals. Cultured kidney epithelial cells from TAZ$^{-/-}$ mice overexpressed PC2 2.2-fold in comparison with cells from $+/-$ and $+/+$ animals, while levels of β-tubulin were unaffected.

Because TAZ is known to function as a transcriptional regulator, we asked whether the overexpression of PC2 might be related to changes in transcription of PKD2 relative to PKD1 in kidneys of TAZ$^{-/-}$ mice. Total RNA extracts from kidneys of $+/+$, $+/-$, and $-/-$ mice at different ages were analyzed by real-time RT-PCR using GAPDH RNA as an internal control.
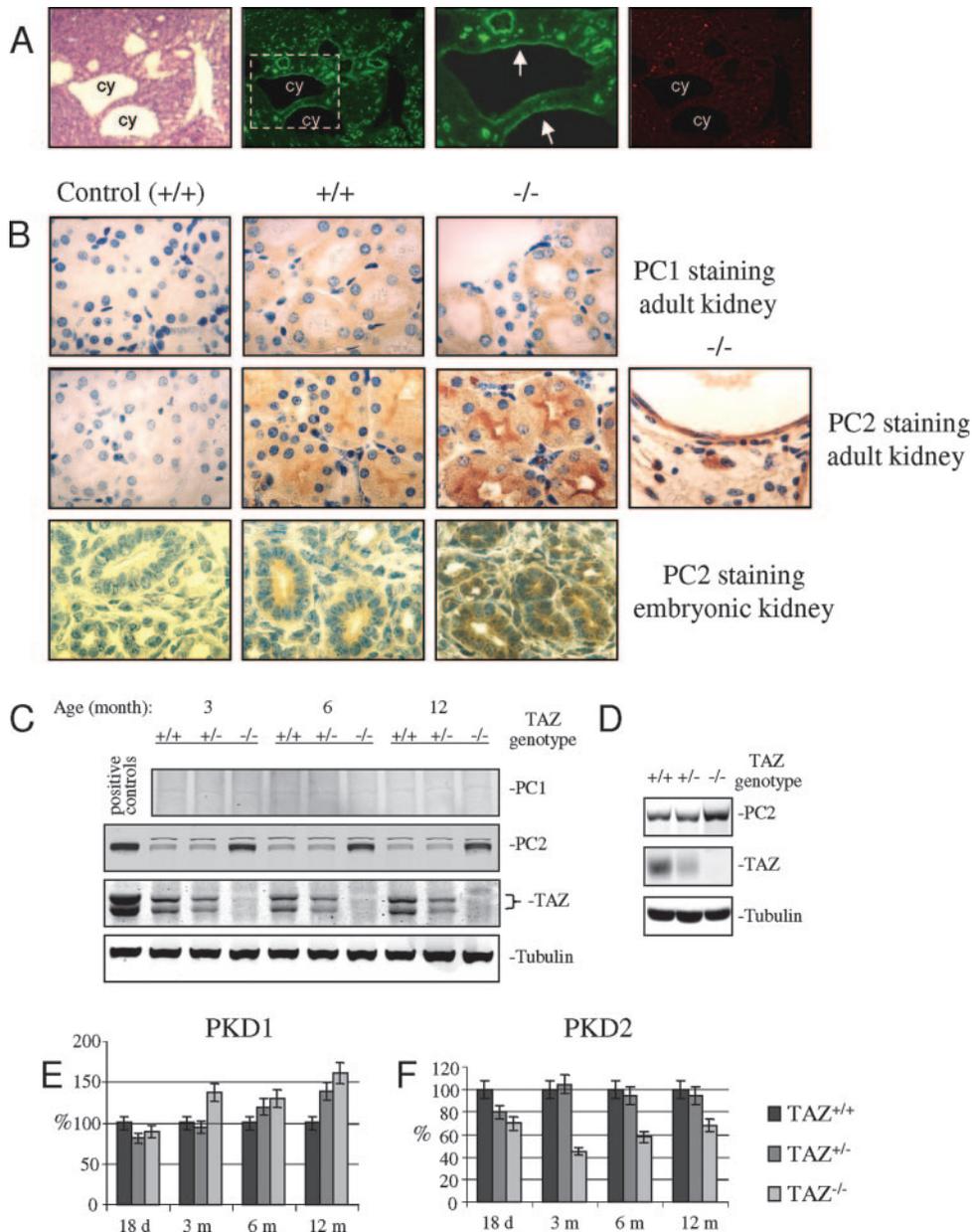
FIG. 2. TAZ affects levels of PC2 expression without an effect on PKD2 RNA levels. (A) Origins of renal cysts in a 2-week-old TAZ$^{-/-}$ mouse. Panels left to right: H&E staining; staining with fluorescein isothiocyanate-coupled *Lotus tetragonolobus* agglutinin as a marker of proximal tubules; higher magnification of the area outlined in second panel with arrows indicating staining of cells lining a cyst; staining of the same section with tetramethyl rhodamine isothiocyanate-coupled DBA as a marker of collecting ducts. (B) Expression levels and localization of PC1 and PC2 in mouse kidneys. Magnification, ×400. Upper panels: staining of kidneys of 3-month-old mice with anti-PC1 antibody (sc-10374; Santa Cruz). Panels left to right: +/+ kidney with normal IgG control, +/+ with anti-PC1; −/− with anti-PC1. Middle panels: staining of kidneys of 3-month-old mice with anti-PC2 antibody 5459. Left to right: +/+ control with antibody preadsorbed with GST-PC2 C-terminal cytoplasmic fragment; +/+ anti-PC2; −/− anti-PC2. Lower panels: embryonic kidneys (14.5 days) with anti-PC2 antibody 5459. Left to right: +/+ with normal IgG control; +/+ anti-PC2; −/− anti-PC2. (C and D) Lysates from mouse kidney tissues (C) and cultured BMK cells (D) from +/+, +/−, and −/− mice were blotted with anti-PC1 (sc-25570; Santa Cruz), anti-PC2 antibody (5459), anti-β-tubulin (T0198; Sigma), and anti-TAZ antibodies. Positive controls are lysates from 293 cells transfected with PC2 and TAZ expression constructs. (E and F) Real-time PCR for PKD1 (E) and PKD2 (F) using total RNA extracts from +/+, +/−, and −/− mouse kidneys at different ages. Results are normalized to GAPDH.

PKD1 mRNA levels were essentially the same in mice of all three genotypes, though slight elevations were seen in older −/− animals (Fig. 2E). Levels of PKD2 mRNA were consistently lower in −/− mice compared to their normal +/+ and +/− littermates (Fig. 2F). Overexpression of PC2 in TAZ$^{-/-}$ mice is therefore not a result of increased steady-state levels of PKD2 mRNA. These results do not support the hypothesis of TAZ as a transcriptional coactivator of PKD2 but rather suggest the possibility that TAZ regulates PC2 levels by some posttranscriptional mechanism.

Control MO   TAZ MO
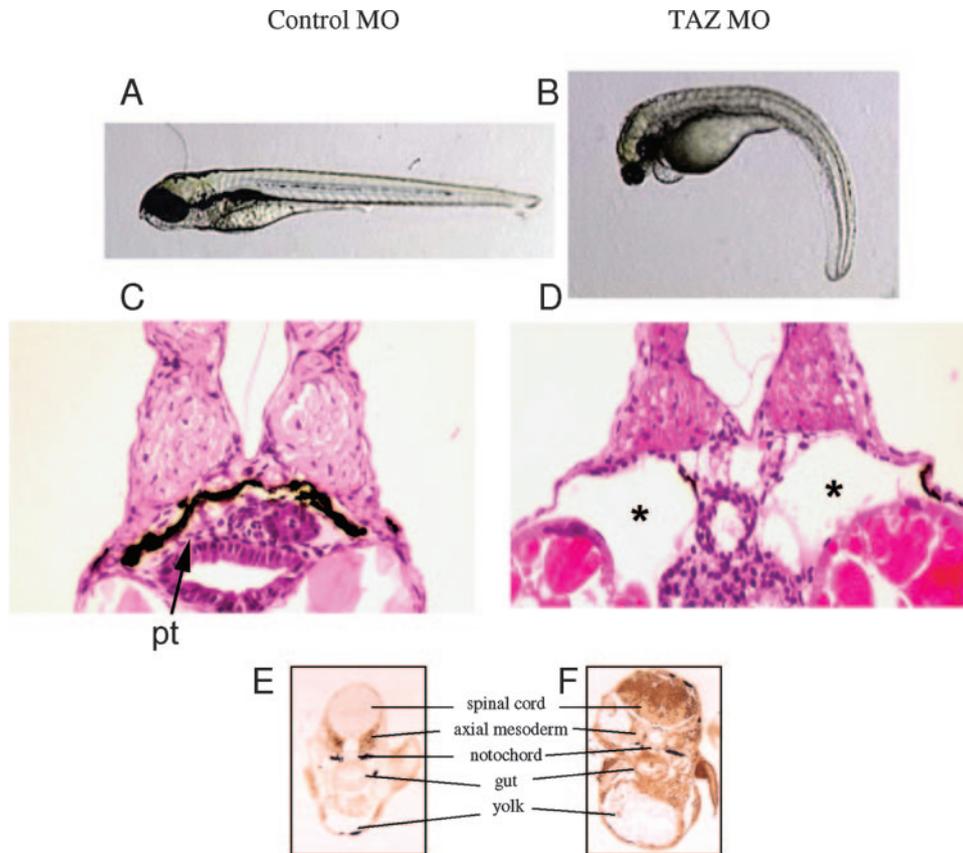
FIG. 3. Downregulation of TAZ in zebrafish embryos results in renal cyst formation and overexpression of PC2. (A and B) Whole mounts of embryos demonstrate pronounced ventral curvature in the TAZ knockdown animal. (C and D) H&E staining showing a pronephric tubule (pt) in the control embryo (C) and corresponding cystic dilatation of the pronephric tubules (asterisk) in the TAZ-depleted embryo (D). (E and F) Staining of saggital sections of the control (E) and TAZ MO (F) with anti-PC2 (antibody 5459) showing elevated PC2 protein levels in the TAZ knockdown mouse.

Ciliary abnormalities have been linked to PKD in human PKD as well as in animal models (7, 18). Immunofluorescent staining with anti-acetylated α-tubulin revealed the presence of cilia in primary kidney epithelial cells from TAZ-deficient as well as normal mice. PC2 was seen to colocalize with cilia in these cells (see Fig. S4A in the supplemental material). TAZ is also found in cilia in wild-type BMK epithelial cells (see Fig. S4B) and in IMCD cells expressing HA-tagged TAZ (see Fig. S4C). Whether cilia in TAZ-deficient mice are of normal size and retain normal function remains unknown.

Depletion of TAZ in zebrafish results in cystic nephron formation and overexpression of PC2. TAZ is 68% identical in the mouse and zebrafish and functions in a similar fashion in directing mesenchymal cell differentiation in the two species (21). To investigate whether normal kidney development in a vertebrate species distant from the mouse shows a similar dependency on TAZ and to further investigate the specific relationship between TAZ deficiency and PKD, a TAZ knockdown was generated in zebrafish. Zebrafish embryos were injected with control or TAZ-specific morpholino oligomers (MO) at the one- to two-cell stage. The normal zebrafish pronephros consists of a fused midline glomerulus drained by two pronephric ducts that shunt the urine outside the animal (13). TAZ knockdown embryos (8 days), in contrast to control mor-

pholino-injected embryos, developed large bilateral cystic dilations in the pronephric tubules (Fig. 3A thru D). The animals also exhibited a body curvature phenotype identical to that seen in other zebrafish cystic kidney gene mutations (57) (Fig. 3A and B). PC2 protein levels were then examined in 3-day embryos treated with the oligomers by using an antibody to the mouse PC2 protein. PC2 expression was elevated throughout the early embryo treated with the TAZ-specific oligomers compared to the control (Fig. 3E and F).

TAZ interacts with PC2 and affects its stability. The effect of TAZ on PC2 protein stability was investigated. 293 (human embryonic kidney) cells were transfected with a construct expressing HA-tagged PC2 with or without TAZ cotransfection, labeled for 6 hours with [^{35}S]methionine, washed, and chased in cold medium for various times. The turnover of metabolically labeled PC2 was clearly accelerated in cells expressing exogenous TAZ. TAZ overexpression reduced the half-life of PC2 by roughly 50% (Fig. 4A). The standard t test comparing the means of triplicate samples with and without exogenous TAZ showed the differences in PC2 decay to be significant ($P = 0.04$). Similar results were obtained using cycloheximide to block protein synthesis and measuring levels of PC2 with or without exogenous TAZ (data not shown). TAZ overexpression also led to enhanced turnover of endogenous PC2 in
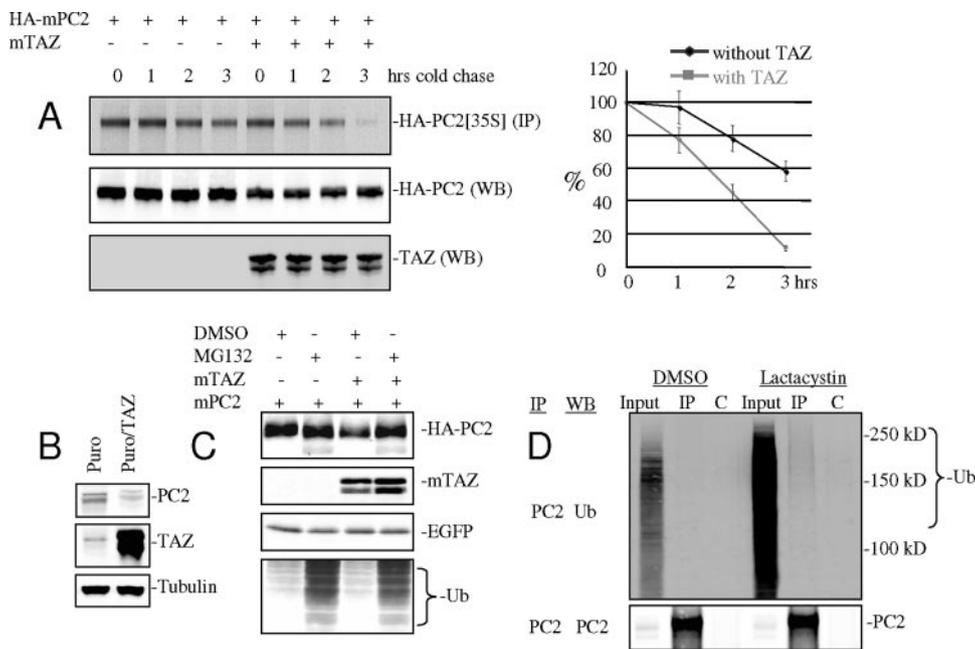
FIG. 4. TAZ promotes PC2 turnover. (A) Pulse-chase experiment in [^{35}S]methionine-labeled 293 cells cotransfected with HA-tagged mPKD2 with TAZ or control vector pcDNA3.1(+). Cells were labeled for 6 h, washed, and incubated further in medium with cold methionine. Cell lysates were made at the indicated times, immunoprecipitated with anti-HA antibody (sc-805; Santa Cruz), and separated by SDS-PAGE. Labeled PC2 protein levels were quantitated by autoradiography and scanning. (B) Established mouse kidney cells of the IMCD line were cotransfected with pMXS-puro plasmid along with a TAZ expression construct or control vector pcDNA3.1(+). After puromycin selection, total cell lysates were separated by SDS-PAGE and blotted for endogenous PC2, TAZ, and tubulin. (C) 293 cells were cotransfected with HA-tagged mPKD2 and pEGFP-N1 along with a TAZ expression construct or control vector pcDNA3.1. Cells were treated with MG132 (5 μM) or dimethyl sulfoxide (DMSO) control for 12 h. Western blot assays for PC2, TAZ, EGFP, and ubiquitin were performed. (D) BMK cells from TAZ$^{+/+}$ mice were treated with lactacystin (5 μM) for 12 h. Cell lysates were made and immunoprecipitation performed under denaturing conditions (1% SDS) using rabbit anti-PC2 antibody 5459. The Western blot for ubiquitin shows that a fraction of PC2 is ubiquitinylated.

IMCD established mouse kidney cells (Fig. 4B). Stability was restored to normal levels by addition of the proteosome inhibitor MG132 (Fig. 4C). Evidence for ubiquitinylation of PC2 in vivo was sought using BMK cells from normal mice cultured with the proteasome inhibitor lactacystin (12, 14). To assess whether PC2 itself and not just coprecipitating proteins were ubiquitinylated, immunoprecipitation was carried out under denaturing conditions (1% SDS) with anti-PC2 and blotted with antiubiquitin antibody. Increased density in the blot suggests that some fraction of PC2 is polyubiquitinylated (Fig. 4D). These results suggest that TAZ regulates PC2 through ubiquitin-dependent proteolysis. Application of a proteasome inhibitor has previously been shown to increase PC2 channel activity (62). The effect of TAZ on PC1 stability was tested in a similar fashion using a C-terminal cytoplasmic fragment of the very large PC1 protein. The PC1 fragment was stable compared to PC2, and its turnover was unaffected by TAZ overexpression (not shown).

Substrates in ubiquitin-dependent degradation are recognized by E3 ligases through protein-protein interactions. A series of TAZ mutants was used to characterize the interaction with PC2. Substitutions of serines 89 and 90 with alanines prevent 14-3-3 binding and lead to accumulation of TAZ in the nucleus (29). As expected from its altered subcellular localization, this mutant showed no detectible interaction with PC2 (Fig. 5B) as well as an inability to promote PC2 degradation (Fig. 5C). Deletion of residues 220 to 272 constituting the CC

(coiled-coil) domain of TAZ strongly reduced binding to PC2 (Fig. 5D), while deletions of the WW and PDZ binding domains had only minor effects (not shown). The cytoplasmic portions of PC1 and PC2 are known to interact through their coiled-coil domains (52, 60). Expression of a C-terminal cytoplasmic fragment of mPC1 (residues 4066 to 4293) prevented TAZ-PC2 interaction (Fig. 5D), indicating that interaction with PC1 spares PC2 from TAZ-mediated degradation. PC2 levels were unaffected by expression of either the ΔCC mutant of TAZ (Fig. 5E) or the cytoplasmic fragment of PC1 (Fig. 5F). The parallel effects of these constructs on binding and turnover of PC2 support the conclusion that interaction between TAZ and PC2 leads to PC2 degradation. TAZ binds to the cytoplasmic domain of PC2 represented by the 289-residue C-terminal fragment (residues 678 to 966) of the protein (Fig. 5A and D). Deletion of the C-terminal 5 amino acids representing a PDZ-binding motif in PC2 diminished TAZ binding, while deletion of the central coiled-coil domain of PC2 (residues 760 to 796) had little or no effect (Fig. 5G). Another unidentified cellular protein, presumably with a PDZ domain, may conceivably be involved in the TAZ-PC2 interaction. TAZ and PC2 interaction in 293 cells was confirmed by immunoprecipitation and GST pull-down using full-length HA-tagged PC2 and a TAZ GST fusion (Fig. 5H and I).

TAZ mediates degradation of PC2 as part of a SCF$^{\beta\text{-Trcp}}$ complex. TAZ contains two consensus phosphodegron motifs for potential β-Trcp binding (64). Substrate phosphorylation is
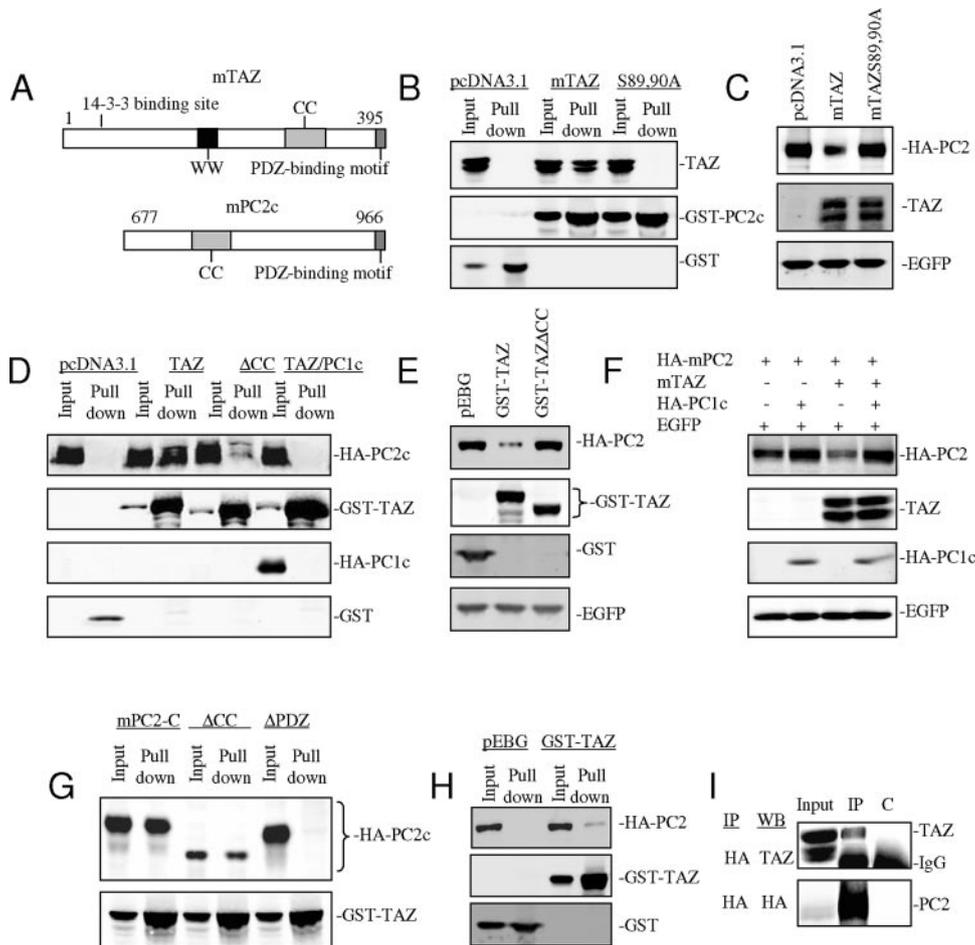
FIG. 5. TAZ interacts with PC2 and promotes its degradation. (A) Schematic of TAZ and the 290-amino-acid C-terminal portion of mouse PC2. (B) 293 cells were transfected with wild-type TAZ or TAZ 14-3-3 binding mutant S89A/S90A along with a GST fusion to the C-terminal portion of PC2 (GST-PC2c). GST pull-down assays and Western blotting show that PC2c pulls down wild-type TAZ. (C) Wild-type and mutant TAZ were cotransfected along with full-length PC2. The Western blot shows that wild-type but not mutant TAZ is able to promote PC2 degradation. (D thru F) PC2-c, GST-TAZ, TAZ coiled-coil region deletion mutant (ΔCC), and PC1 C-terminal cytoplasmic fragment (residues 4066 to 4293; PC1c) were cotransfected into 293 cells as indicated. GST pull-down assays and Western blotting show that GST-TAZ but not the ΔCC mutant interacts with PC2c and that GST-TAZ/PC2c interaction is inhibited by coexpression of PC1c (D). The Western blot shows that the ΔCC TAZ mutant is ineffective in promoting degradation of PC2 (E). HA-tagged PC2, TAZ, PC1c, and EGFP were cotransfected into 293 cells as indicated. The Western blot shows that PC1c stabilizes PC2 and blocks TAZ-mediated PC2 degradation (F). (G) GST-TAZ, HA-tagged PC2c and mutants were cotransfected into 293 cells as indicated. GST pull-down assay and Western blotting show that the C-terminal 5 amino acids of PC2 resembling a PDZ-binding motif is important for the PC2c/GST-TAZ interaction. (H) GST pull down was performed on an extract of 293 cells transfected with cDNAs of GST-mTAZ and full-length mPC2. The Western blot shows full-length PC2 associated with GST-TAZ. (I) Immunoprecipitation was performed on an extract of 293 cells transfected with cDNAs of mTAZ and HA-tagged mPC2. The Western blot shows association of TAZ with HA-PC2.

a key to the specificity of SCF$^{\beta\text{-Trcp}}$ E3 ligase complexes (3), and both TAZ (29) and PC2 (6) are known to be phosphorylated. To investigate whether TAZ mediates PC2 degradation directly as part of an SCF$^{\beta\text{-Trcp}}$ E3 ligase complex, dominant-negative constructs of Cul1 and Trcp were introduced into 293 cells along with TAZ and PC2. TAZ-mediated degradation of PC2 was prevented by coexpression of Cul1DN and by the F-box deletion mutant of β-Trcp (Fig. 6A). The cyclin-cdk inhibitor p27 (8, 61) as a known target of Cul1 and cdc25A as a known target of Cul1 and β-Trcp (5, 28) were used as positive controls. Targeting endogenous β-Trcp in 293 cells with siRNA constructs was effective in preventing TAZ-mediated PC2 degradation (Fig. 6B). These results implicate TAZ in a SCF$^{\beta\text{-Trcp}}$ pathway that targets PC2.

Further evidence that TAZ forms part of an SCF$^{\beta\text{-Trcp}}$ complex was sought by GST pull-down and coimmunoprecipitation experiments. Endogenous Cul1 was pulled down from extracts of 293 cells transfected with GST-TAZ (see Fig. S5A in the supplemental material). Anti-Cul1 was used to bring down TAZ from the same cell extracts (see Fig. S5B in the supplemental material). Myc-tagged β-Trcp1 and β-Trcp2 were cotransfected along with GST-TAZ into 293 cells. GST pull-down and coimmunoprecipitation showed interaction in both directions between TAZ and the two β-Trcp isoforms (see Fig. S5C and D in the supplemental material). As expected, PC2 also associates with β-Trcp. Interaction was confirmed by coimmunoprecipitation and Western blotting using epitope-tagged constructs (see Fig. S5E and F in the supplemental
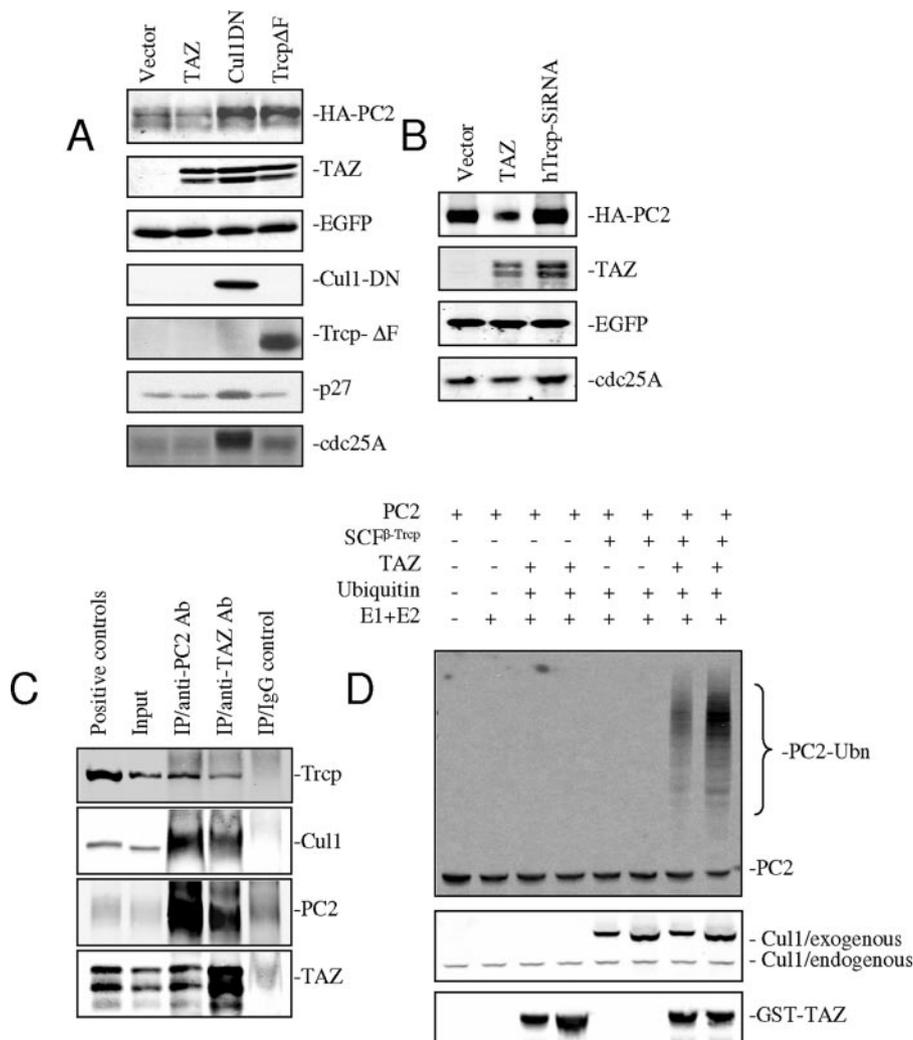
FIG. 6. TAZ mediates PC2 turnover as part of an SCF$^{\beta\text{-Trcp}}$ E3 ligase complex. (A) HA-tagged mPKD2 and TAZ were cotransfected along with dominant negative constructs of Cul1 (CulDN) and Trcp (TrcpΔF) in 293 cells along with EGFP as a transfection control. The Western blot shows that expression of either CulDN or TrcpΔF prevents TAZ-mediated PC2 degradation. p27 and cdc25A were used as positive controls for disruption by Cul1- and β-Trcp-dependent pathways, respectively. (B) TAZ and mPKD2 cDNAs were cotransfected into 293 cells along with a β-Trcp siRNA construct specific for human β-Trcp. The Western blot shows that PC2 degradation is blocked by β-Trcp siRNA. (C) Immuno-precipitation was performed using anti-PC2 and TAZ antibodies and IMCD cell lysates. Western blots show that TAZ and PC2 associate with endogenous Cul1 and β-Trcp. (D) PC2 ubiquitylation was performed using in vitro-translated ^{35}S-labeled PC2 in the presence of TAZ and SCF$^{\beta\text{-Trcp}}$ E3 ligase complex. Autoradiography shows that PC2 can be ubiquinylated in vitro in the presence of TAZ and SCF$^{\beta\text{-Trcp}}$ E3 ligase.

material). Expression of the C-terminal fragment of PC1 slightly reduced the amount of PC2 associated with β-Trcp (see Fig. S5G in the supplemental material), consistent with the inhibition of TAZ-PC2 interaction by this PC1 fragment (Fig. 5F and H). The associations between TAZ, PC2, Cul1, and β-Trcp as endogenous proteins were confirmed using IMCD cells. Coimmunoprecipitation was performed on IMCD cell lysates using anti-PC2 and anti-TAZ antibodies. Cul1 and β-Trcp were brought down with both antibodies but not with normal IgG (Fig. 6C).

TAZ- and SCF$^{\beta\text{-Trcp}}$-dependent ubiquitinylation of PC2 were confirmed in an in vitro assay. SCF$^{\beta\text{-Trcp}}$ complex and TAZ from 293 cells were incubated with in vitro-translated ^{35}S-labeled PC2 along with E1, E2, and ubiquitin. A portion of the labeled PC2 migrates as high-molecular-weight species

when TAZ and SCF$^{\beta\text{-Trcp}}$ E3 ligase complex are present but not in control lanes (Fig. 6D). These results indicate that PC2 is ubiquitinylated by SCF$^{\beta\text{-Trcp}}$ E3 ligase in a TAZ-dependent manner.

To investigate whether either the N-terminal (DS$_{58}$GSHS$_{62}$) or C-terminal (S$_{302}$REQS$_{306}$TDS$_{309}$GLG) phosphodegron motif in TAZ (Fig. 7, top) is involved in β-Trcp binding and plays a role in PC2 turnover, serine-to-alanine substitutions were introduced into each of the sites and the constructs expressed in 293 cells. Substitution of serine 309 in the C-terminal motif led to loss of β-Trcp binding, while substitutions in the N-terminal site had no effect (Fig. 7A). To investigate further if other serines near the C-terminal β-Trcp binding site in TAZ may be important, S306A and S302A mutants were made and analyzed. The results show the importance of S306
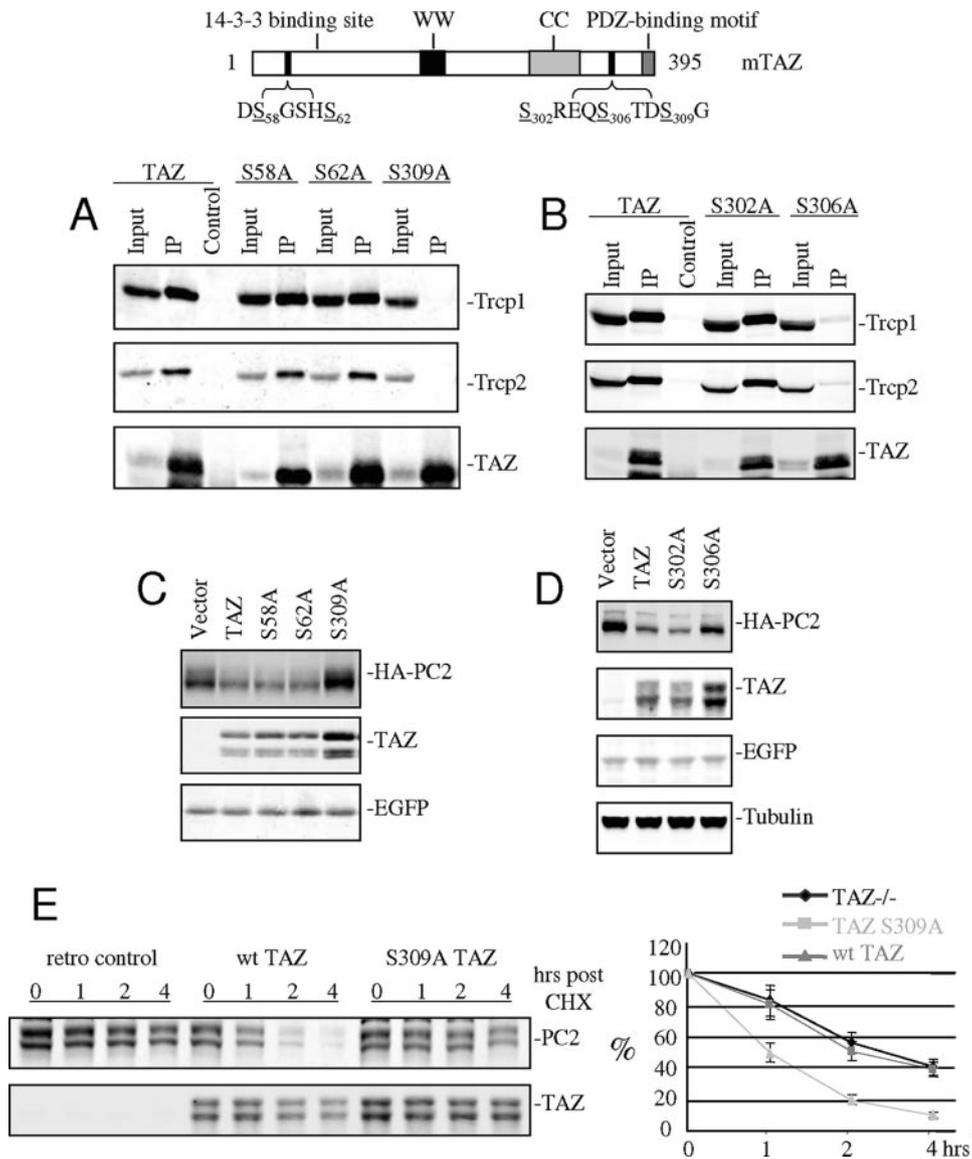
FIG. 7. Serines 306 and 309 of TAZ are important for TAZ-mediated PC2 degradation. Top: schematic showing sequences of two phospho-degron-like motifs in TAZ. (A and B) cDNAs of wild-type TAZ and TAZ mutants containing serine-to-alanine substitutions were cotransfected along with myc-tagged β-Trcp isoforms into 293 cells. Immunoprecipitation and Western blotting show that the S306A and S309A mutants have lost the ability to bind β-Trcp. (C and D) cDNAs of HA-mPC2, EGFP, and TAZ mutants were cotransfected into 293 cells. The Western blot shows that mutants S306A and S309A have lost the ability to promote PC2 degradation. (E) TAZ$^{-/-}$ MEFs were infected with control, wild type, or S309A mutant TAZ retroviruses. Cells were treated with cycloheximide (CHX; 20 μg/ml) at 24 h postinfection and extracted at the indicated times following CHX addition. Introduction of the wild-type but not mutant S309A TAZ increased the rate of PC2 degradation.

and not of S302 (Fig. 7B). In terms of effects on PC2 stability, substitution of serines 309 and 306 with alanine in the C-terminal motif blocked TAZ-mediated PC2 degradation (Fig. 7C and D), consistent with their failure to bind β-Trcp. TAZ therefore links PC2 to a SCF$^{β-Trcp}$ E3 ligase complex through its C-terminal β-Trcp binding site. Endogenous PC2 expression and stability were also examined in TAZ$^{-/-}$ MEFs infected by control and TAZ-transducing retroviruses. The expression level and half-life of PC2 were reduced by roughly 50% when wild-type TAZ was introduced (differences were significant by t test, $P = 0.03$). Infection of TAZ$^{-/-}$ with the retrovirus encoding the S309A TAZ mutant failed to promote

PC2 degradation (Fig. 7E), confirming the results shown in transfected 293 cells (Fig. 7A). It is also apparent that the turnover of TAZ itself is regulated in the SCF$^{β-Trcp}$ complex dependent on the same phosphodegron sequences as is evident in the Western blots in Fig. 6B and 7C and D.

DISCUSSION

The present studies of a TAZ knockout mouse have uncovered a novel biological and molecular function of the TAZ protein as a component of an SCF$^{β-Trcp}$ E3 ligase complex. Studies primarily in cell culture systems have established TAZ
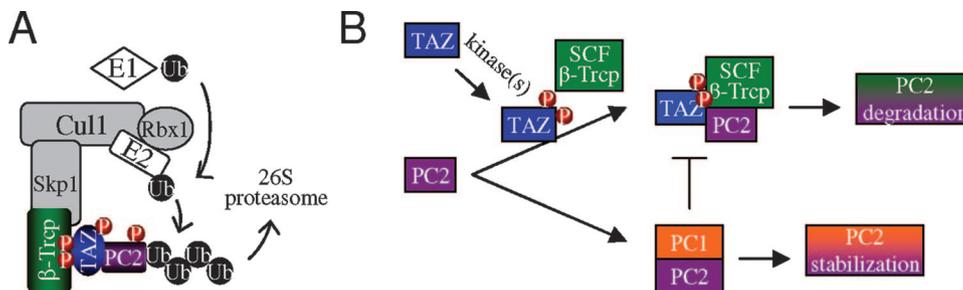
FIG. 8. Model of TAZ-mediated PC2 protein degradation. (A) TAZ uses its C-terminal phosphodegron motif to link PC2 to an SCF$^{\beta\text{-Trcp}}$ E3 ligase complex. (B) PC2 degradation is regulated by TAZ phosphorylation. Interaction of PC2 with PC1 protects PC2 from TAZ-mediated degradation.

as a transcriptional regulator with a variety of roles in cellular differentiation (9, 21, 29, 40, 41, 45). The TAZ protein is found in the cytoplasm as well as the nucleus, its distribution governed by phosphorylation and binding to 14-3-3 (29). A central WW domain and a coiled-coiled domain in TAZ are also critical to its role as a transcriptional regulator (9, 21, 29, 40, 41, 45). TAZ is multiply phosphorylated. It is found in complexes with PP2A and undergoes dephosphorylation in polyomavirus-infected cells with important consequences for virus growth and cell transformation (59). The dual functions of TAZ as a regulator of protein degradation and transcription places it with E6-AP, which also possesses both transcriptional regulatory (44) and E3 ligase (25) functions. TAZ and E6AP also share the property of being targeted by oncoproteins encoded by DNA tumor viruses of the polyoma (59) and papilloma groups (24).

TAZ deficiency results in a partial embryonic lethal phenotype with roughly half of the $-/-$ embryos dying in utero. The cause of prenatal deaths in these embryos has not been investigated but may be related to the role of TAZ in mesenchymal stem cell differentiation (21). Surviving TAZ$^{-/-}$ pups are runted but produce histologically normal bone and fat. These mice show severe abnormalities in kidneys and lungs. The development of multiple cysts in the kidneys of these animals resembles the changes seen in human polycystic kidney disease. TAZ knockout mice also develop emphysema, raising the possibility that TAZ deficiency may result in abnormal accumulation of a specific protein(s) in the lung. Abnormalities in kidney and lung were seen in 100% of TAZ$^{-/-}$ mice, indicating the importance of TAZ in maintaining normal ductal and alveolar structures.

These results correlate well with those in an independent study of a TAZ knockout mouse (22) with respect to the major histopathological finding of PKD. Development of renal cysts constitutes the most significant finding in both mice, though some differences may exist regarding the origin and distribution of cysts within the nephron. The findings are also in agreement with respect to the absence of any major skeletal defects or manifestations of abnormal mesenchymal cell differentiation. An important difference between the two models exists with respect to involvement of the lung. Severe emphysema developed along with PKD in 100% of our TAZ$^{-/-}$ mice, whereas no involvement of the lung was reported in the earlier study. TAZ has been shown to affect levels of surfactant C through binding to TTF-1 (45). Based on its role as a compo-

nent of an E3 ligase, TAZ may possibly regulate the levels of other surfactants or factors essential for alveolar integrity through its protein degradation function. In contrast to the partial embryonic lethality in our mice, their TAZ$^{-/-}$ mice were born in the expected Mendelian ratios with up to half succumbing by the age of weaning. The expression levels of several genes linked to ciliary function and cystic disease were found to be lower in their knockout mouse, consistent with TAZ as a possible transcriptional regulator of those genes. The present results have uncovered another molecular mechanism that may contribute to PKD based on the role of TAZ in protein degradation.

Comparisons of renal disease in TAZ knockout mice with other well-studied mouse models of cystic kidney disease show some clinical and pathological differences as well as similarities. In models involving *cpk* (16, 50), *jcpk* (15, 19), and DBA/2-*pcy* (58), cysts vary in their time course of development, but the entire renal cortex is ultimately replaced by cystic tubules and the kidneys become massively enlarged. Cortical cysts also develop increasingly with age in TAZ$^{-/-}$ mice. Defects in ciliagenesis have been found in some animal models of PKD (7, 18). A number of genes affecting cyst formation in the zebrafish kidney have been identified and shown to be involved in the development and function of cilia (57). TAZ is expressed on cilia in normal kidney epithelial cells. The absence of TAZ does not prevent formation of cilia per se.

PC1 and PC2 are the two proteins altered in the autosomal dominant forms of human PKD through mutations in PKD1 and PKD2 (30, 49). Animal models of PKD have been described based on alterations in expression of PC1 or PC2. In both the human and experimental animals, PKD is associated with alterations in the ratio of these interacting proteins. The current study has shown that TAZ functions as a β-Trcp-binding protein in an E3-ubiquitin ligase complex that targets PC2 for degradation and that PC2 accumulates abnormally in kidneys of TAZ-deficient mice. TAZ contains a phosphodegron motif recognized by the F-box protein β-Trcp. Phosphorylation of this motif by an unknown kinase(s) results in β-Trcp binding and incorporation of TAZ into an SCF$^{\beta\text{-Trcp}}$ ligase complex that also contains PC2. PC2 is overexpressed roughly twofold in kidney epithelial cells of TAZ$^{-/-}$ mice. The accumulation of PC2 is not due to increased transcription of PKD2 but rather to the absence of the protein degradation function of TAZ. The latter conclusion is supported by results of experiments carried out in 293 human embryonic kidney

cells showing that overexpression of TAZ leads to more rapid turnover of PC2 via a β-Trcp-E3 ubiquitin ligase pathway. The importance of TAZ phosphorylation in mediating degradation of PC2 has been confirmed using TAZ$^{-/-}$ MEFs restored with either wild-type or mutant forms of TAZ altered in one of its phosphodegron motifs. Figure 8A and B is a schematic representation of the findings on the new function of TAZ as an adaptor protein in an SCF$^{β-Trcp}$ ligase complex.

An imbalance between PC1 and PC2 may be expected to affect the ion transport functions of the polycystin complex. Epithelial cells from PKD1 knockout mice fail to respond to fluid flow (42), and reduced expression of PC1 results in PKD (33). Overexpression of PC1 in transgenic mice also results in the development of PKD (51), akin to the observations in the TAZ knockout mouse with overexpression of PC2. Overexpression of PC2 may have consequences in terms of the interactions of these critical proteins and their coupling to G proteins (10, 11, 46) and downstream Ca^{2+} signaling (10, 17, 20, 36, 62). Increased levels of PC2 by itself in the endoplasmic reticulum can lead to release of excess Ca^{2+} into the cytosol (31, 32) with potentially severe consequences. Previous studies have shown that when overexpressed PC2 accumulates in the endoplasmic reticulum and increases Ca^{2+} entry (36).

A knockdown of TAZ in the zebrafish embryo results in cyst formation in the pronephros and in overexpression of PC2 throughout the embryo. These findings duplicate basic features of the TAZ knockout mouse and reveal a remarkable evolutionary conservation of TAZ functions at the molecular and development levels. The present investigation has focused on PC2 overexpression in order to identify a new molecular function of TAZ. While PC2 overaccumulation may be a contributory factor in the development of PKD, other factors regulated by TAZ are likely to be involved. Through its functions either in transcription or protein degradation or both, TAZ may alter the levels of any of a number of proteins involved in the assembly and function of primary cilia. Variations in age of onset and rate of progression in ADPKD are consistent with the existence of modifying environmental or genetic factors. The "two-hit" theory is widely accepted as a mechanism for cyst formation in ADPKD (54). Somatic mutations affecting the normal alleles in PKD1 or PKD2 are known to occur in some cysts (48, 53, 65). The present results call for further investigation of TAZ as a possible modifier or "second hit" in ADPKD.

ACKNOWLEDGMENTS

REFERENCES

1. **Ahn, M. Y., S. C. Bae, M. Maruyama, and Y. Ito.** 1996. Comparison of the human genomic structure of the Runt domain-encoding PEBP2/CBFα gene family. Gene **168:**279–280.

2. **Amsterdam, A., S. Burgess, G. Golling, W. Chen, Z. Sun, K. Townsend, S. Farrington, M. Haldi, and N. Hopkins.** 1999. A large-scale insertional mutagenesis screen in zebrafish. Genes Dev. **13:**2713–2724.

3. **Bai, C., P. Sen, K. Hofmann, L. Ma, M. Goebl, J. W. Harper, and S. J. Elledge.** 1996. SKP1 connects cell cycle regulators to the ubiquitin proteolysis machinery through a novel motif, the F-box. Cell **86:**263–274.

4. **Bhunia, A. K., K. Piontek, A. Boletta, L. Liu, F. Qian, P. N. Xu, F. J. Germino, and G. G. Germino.** 2002. PKD1 induces p21^{waf1} and regulation of the cell cycle via direct activation of the JAK-STAT signaling pathway in a process requiring PKD2. Cell **109:**157–168.

5. **Busino, L., M. Donzelli, M. Chiesa, D. Guardavaccaro, D. Ganoth, N. V. Dorrello, A. Hershko, M. Pagano, and G. F. Draetta.** 2003. Degradation of Cdc25A by β-TrCP during S phase and in response to DNA damage. Nature **426:**87–91.

6. **Cai, Y., G. Anyatonwu, D. Okuhara, K. B. Lee, Z. Yu, T. Onoe, C. L. Mei, Q. Qian, L. Geng, R. Wiztgall, B. E. Ehrlich, and S. Somlo.** 2004. Calcium dependence of polycystin-2 channel activity is modulated by phosphorylation at Ser812. J. Biol. Chem. **279:**19987–19995.

7. **Calvet, J. P.** 2002. Cilia in PKD—letting it all hang out. J. Am. Soc. Nephrol. **13:**2614–2616.

8. **Carrano, A. C., E. Eytan, A. Hershko, and M. Pagano.** 1999. SKP2 is required for ubiquitin-mediated degradation of the CDK inhibitor p27. Nat. Cell Biol. **1:**193–199.

9. **Cui, C. B., L. F. Cooper, X. Yang, G. Karsenty, and I. Aukhil.** 2003. Transcriptional coactivation of bone-specific transcription factor Cbfa1 by TAZ. Mol. Cell. Biol. **23:**1004–1013.

10. **Delmas, P., S. M. Nauli, X. Li, B. Coste, N. Osorio, M. Crest, D. A. Brown, and J. Zhou.** 2004. Gating of the polycystin ion channel signaling complex in neurons and kidney cells. FASEB J. **18:**740–742.

11. **Delmas, P., H. Nomura, X. Li, M. Lakkis, Y. Luo, Y. Segal, J. M. Fernandez-Fernandez, P. Harris, A. M. Frischauf, D. A. Brown, and J. Zhou.** 2002. Constitutive activation of G-proteins by polycystin-1 is antagonized by polycystin-2. J. Biol. Chem. **277:**11276–11283.

12. **Dick, L. R., A. A. Cruikshank, L. Grenier, F. D. Melandri, S. L. Nunes, and R. L. Stein.** 1996. Mechanistic studies on the inactivation of the proteasome by lactacystin: a central role for clasto-lactacystin β-lactone. J. Biol. Chem. **271:**7273–7276.

13. **Drummond, I. A., A. Majumdar, H. Hentschel, M. Elger, L. Solnica-Krezel, A. F. Schier, S. C. Neuhauss, D. L. Stemple, F. Zwartkruis, Z. Rangini, W. Driever, and M. C. Fishman.** 1998. Early development of the zebrafish pronephros and analysis of mutations affecting pronephric function. Development **125:**4655–4667.

14. **Fenteany, G., R. F. Standaert, W. S. Lane, S. Choi, E. J. Corey, and S. L. Schreiber.** 1995. Inhibition of proteasome activities and subunit-specific amino-terminal threonine modification by lactacystin. Science **268:**726–731.

15. **Flaherty, L., E. C. Bryda, D. Collins, U. Rudofsky, and J. C. Montogomery.** 1995. New mouse model for polycystic kidney disease with both recessive and dominant gene effects. Kidney Int. **47:**552–558.

16. **Fry, J. L., Jr., W. E. Koch, J. C. Jennette, E. McFarland, F. A. Fried, and J. Mandell.** 1985. A genetically determined murine model of infantile polycystic kidney disease. J. Urol. **134:**828–833.

17. **Gonzalez-Perrett, S., K. Kim, C. Ibarra, A. E. Damiano, E. Zotta, M. Batelli, P. C. Harris, I. L. Reisin, M. A. Arnaout, and H. F. Cantiello.** 2001. Polycystin-2, the protein mutated in autosomal dominant polycystic kidney disease (ADPKD), is a Ca^{2+}-permeable nonselective cation channel. Proc. Natl. Acad. Sci. USA **98:**1182–1187.

18. **Guay-Woodford, L. M.** 2003. Murine models of polycystic kidney disease: molecular and therapeutic insights. Am. J. Physiol. Renal Physiol. **285:** F1034–F1049.

19. **Guay-Woodford, L. M., E. C. Bryda, B. Christine, J. R. Lindsey, W. R. Collier, E. D. Avner, P. D'Eustachio, and L. Flaherty.** 1996. Evidence that two phenotypically distinct mouse PKD mutations, bpk and jcpk, are allelic. Kidney Int. **50:**1158–1165.

20. **Hanaoka, K., F. Qian, A. Boletta, A. K. Bhunia, K. Piontek, L. Tsiokas, V. P. Sukhatme, W. B. Guggino, and G. G. Germino.** 2000. Co-assembly of polycystin-1 and -2 produces unique cation-permeable currents. Nature **408:**990–994.

21. **Hong, J. H., E. S. Hwang, M. T. McManus, A. Amsterdam, Y. Tian, R. Kalmukova, E. Mueller, T. Benjamin, B. M. Spiegelman, P. A. Sharp, N. Hopkins, and M. B. Yaffe.** 2005. TAZ, a transcriptional modulator of mesenchymal stem cell differentiation. Science **309:**1074–1078.

22. **Hossain, Z., S. M. Ali, H. L. Ko, J. Xu, C. P. Ng, K. Guo, Z. Qi, S. Ponniah, W. Hong, and W. Hunziker.** 2007. Glomerulocystic kidney disease in mice with a targeted inactivation of Wwtr1. Proc. Natl. Acad. Sci. USA **104:**1631–1636.

23. **Hughes, J., C. J. Ward, B. Peral, R. Aspinwall, K. Clark, J. L. San Millan, V. Gamble, and P. C. Harris.** 1995. The polycystic kidney disease 1 (PKD1) gene encodes a novel protein with multiple cell recognition domains. Nat. Genet. **10:**151–160.

24. **Huibregtse, J. M., M. Scheffner, and P. M. Howley.** 1991. A cellular protein mediates association of p53 with the E6 oncoprotein of human papillomavirus types 16 or 18. EMBO J. **10:**4129–4135.

25. **Huibregtse, J. M., M. Scheffner, and P. M. Howley.** 1993. Localization of the E6-AP regions that direct human papillomavirus E6 binding, association with p53, and ubiquitination of associated proteins. Mol. Cell. Biol. **13:**4918–4927.

26. **International Polycystic Kidney Disease Consortium.** 1995. Polycystic kidney disease: the complete structure of the PKD1 gene and its protein. Cell **81:**289–298.

27. **Ito, Y.** 1989. Signals and transcription factors. Gan To Kagaku Ryoho **16:**509–515. (In Japanese.)

28. **Jin, J., T. Shirogane, L. Xu, G. Nalepa, J. Qin, S. J. Elledge, and J. W. Harper.** 2003. SCFβ-TRCP links Chk1 signaling to degradation of the Cdc25A protein phosphatase. Genes Dev. **17:**3062–3074.

29. **Kanai, F., P. A. Marignani, D. Sarbassova, R. Yagi, R. A. Hall, M. Donowitz, A. Hisaminato, T. Fujiwara, Y. Ito, L. C. Cantley, and M. B. Yaffe.** 2000. TAZ: a novel transcriptional co-activator regulated by interactions with 14-3-3 and PDZ domain proteins. EMBO J. **19:**6778–6791.

30. **Kimberling, W. J., P. R. Fain, J. B. Kenyon, D. Goldgar, E. Sujansky, and P. A. Gabow.** 1988. Linkage heterogeneity of autosomal dominant polycystic kidney disease. N. Engl. J. Med. **319:**913–918.

31. **Koulen, P., Y. Cai, L. Geng, Y. Maeda, S. Nishimura, R. Witzgall, B. E. Ehrlich, and S. Somlo.** 2002. Polycystin-2 is an intracellular calcium release channel. Nat. Cell Biol. **4:**191–197.

32. **Koulen, P., R. S. Duncan, J. Liu, N. E. Cohen, J. A. Yannazzo, N. McClung, C. L. Lockhart, M. Branden, and M. Buechner.** 2005. Polycystin-2 accelerates Ca^{2+} release from intracellular stores in Caenorhabditis elegans. Cell Calcium **37:**593–601.

33. **Lantinga-van Leeuwen, I. S., J. G. Dauwerse, H. J. Baelde, W. N. Leonhard, A. van de Wal, C. J. Ward, S. Verbeek, M. C. Deruiter, M. H. Breuning, E. de Heer, and D. J. Peters.** 2004. Lowering of Pkd1 expression is sufficient to cause polycystic kidney disease. Hum. Mol. Genet. **13:**3069–3077.

34. **Li, Q. L., K. Ito, C. Sakakura, H. Fukamachi, K. Inoue, X. Z. Chi, K. Y. Lee, S. Nomura, C. W. Lee, S. B. Han, H. M. Kim, W. J. Kim, H. Yamamoto, N. Yamashita, T. Yano, T. Ikeda, S. Itohara, J. Inazawa, T. Abe, A. Hagiwara, H. Yamagishi, A. Ooe, A. Kaneda, T. Sugimura, T. Ushijima, S. C. Bae, and Y. Ito.** 2002. Causal relationship between the loss of RUNX3 expression and gastric cancer. Cell **109:**113–124.

35. **Lund, A. H., and M. van Lohuizen.** 2002. RUNX: a trilogy of cancer genes. Cancer Cell **1:**213–215.

36. **Luo, Y., P. M. Vassilev, X. Li, Y. Kawanabe, and J. Zhou.** 2003. Native polycystin 2 functions as a plasma membrane Ca^{2+}-permeable cation channel in renal epithelia. Mol. Cell. Biol. **23:**2600–2607.

37. **Mahoney, W. M., Jr., J. H. Hong, M. B. Yaffe, and I. K. Farrance.** 2005. The transcriptional co-activator TAZ interacts differentially with transcriptional enhancer factor-1 (TEF-1) family members. Biochem. J. **388:**217–225.

38. **Mochizuki, T., G. Wu, T. Hayashi, S. L. Xenophontos, B. Veldhuisen, J. J. Saris, D. M. Reynolds, Y. Cai, P. A. Gabow, A. Pierides, W. J. Kimberling, M. H. Breuning, C. C. Deltas, D. J. Peters, and S. Somlo.** 1996. PKD2, a gene for polycystic kidney disease that encodes an integral membrane protein. Science **272:**1339–1342.

39. **Morita, S., T. Kojima, and T. Kitamura.** 2000. Plat-E: an efficient and stable system for transient packaging of retroviruses. Gene Ther. **7:**1063–1066.

40. **Murakami, M., M. Nakagawa, E. N. Olson, and O. Nakagawa.** 2005. A WW domain protein TAZ is a critical coactivator for TBX5, a transcription factor implicated in Holt-Oram syndrome. Proc. Natl. Acad. Sci. USA **102:**18034–18039.

41. **Murakami, M., J. Tominaga, R. Makita, Y. Uchijima, Y. Kurihara, O. Nakagawa, T. Asano, and H. Kurihara.** 2006. Transcriptional activity of Pax3 is co-activated by TAZ. Biochem. Biophys. Res. Commun. **339:**533–539.

42. **Nauli, S. M., F. J. Alenghat, Y. Luo, E. Williams, P. Vassilev, X. Li, A. E. Elia, W. Lu, E. M. Brown, S. J. Quinn, D. E. Ingber, and J. Zhou.** 2003. Polycystins 1 and 2 mediate mechanosensation in the primary cilium of kidney cells. Nat. Genet. **33:**129–137.

43. **Nauli, S. M., and J. Zhou.** 2004. Polycystins and mechanosensation in renal and nodal cilia. Bioessays **26:**844–856.

44. **Nawaz, Z., D. M. Lonard, C. L. Smith, E. Lev-Lehman, S. Y. Tsai, M. J. Tsai, and B. W. O'Malley.** 1999. The Angelman syndrome-associated protein, E6-AP, is a coactivator for the nuclear hormone receptor superfamily. Mol. Cell. Biol. **19:**1182–1189.

45. **Park, K. S., J. A. Whitsett, T. Di Palma, J. H. Hong, M. B. Yaffe, and M. Zannini.** 2004. TAZ interacts with TTF-1 and regulates expression of surfactant protein-C. J. Biol. Chem. **279:**17384–17390.

46. **Parnell, S. C., B. S. Magenheimer, R. L. Maser, C. A. Zien, A. M. Frischauf,** and J. P. Calvet. 2002. Polycystin-1 activation of c-Jun N-terminal kinase and AP-1 is mediated by heterotrimeric G proteins. J. Biol. Chem. **277:**19566–19572.

47. **Pazour, G. J., B. L. Dickert, Y. Vucica, E. S. Seeley, J. L. Rosenbaum, G. B. Witman, and D. G. Cole.** 2000. Chlamydomonas IFT88 and its mouse homologue, polycystic kidney disease gene tg737, are required for assembly of cilia and flagella. J. Cell Biol. **151:**709–718.

48. **Pei, Y., T. Watnick, N. He, K. Wang, Y. Liang, P. Parfrey, G. Germino, and P. St. George-Hyslop.** 1999. Somatic PKD2 mutations in individual kidney and liver cysts support a "two-hit" model of cystogenesis in type 2 autosomal dominant polycystic kidney disease. J. Am. Soc. Nephrol. **10:**1524–1529.

49. **Peters, D. J., and L. A. Sandkuijl.** 1992. Genetic heterogeneity of polycystic kidney disease in Europe. Contrib. Nephrol. **97:**128–139.

50. **Preminger, G. M., W. E. Koch, F. A. Fried, E. McFarland, E. D. Murphy, and J. Mandell.** 1982. Murine congenital polycystic kidney disease: a model for studying development of cystic disease. J. Urol. **127:**556–560.

51. **Pritchard, L., J. A. Sloane-Stanley, J. A. Sharpe, R. Aspinwall, W. Lu, V. Buckle, L. Strmecki, D. Walker, C. J. Ward, C. E. Alpers, J. Zhou, W. G. Wood, and P. C. Harris.** 2000. A human PKD1 transgene generates functional polycystin-1 in mice and is associated with a cystic phenotype. Hum. Mol. Genet. **9:**2617–2627.

52. **Qian, F., F. J. Germino, Y. Cai, X. Zhang, S. Somlo, and G. G. Germino.** 1997. PKD1 interacts with PKD2 through a probable coiled-coil domain. Nat. Genet. **16:**179–183.

53. **Qian, F., T. J. Watnick, L. F. Onuchic, and G. G. Germino.** 1996. The molecular basis of focal cyst formation in human autosomal dominant polycystic kidney disease type I. Cell **87:**979–987.

54. **Reeders, S. T.** 1992. Multilocus polycystic disease. Nat. Genet. **1:**235–237.

55. **Satake, M., T. Ibaraki, Y. Yamaguchi, and Y. Ito.** 1989. Loss of responsiveness of an AP1-related factor, PEBP1, to 12-*O*-tetradecanoylphorbol-13-acetate after transformation of NIH 3T3 cells by the Ha-ras oncogene. J. Virol. **63:**3669–3677.

56. **Shao, X., J. E. Johnson, J. A. Richardson, T. Hiesberger, and P. Igarashi.** 2002. A minimal Ksp-cadherin promoter linked to a green fluorescent protein reporter gene exhibits tissue-specific expression in the developing kidney and genitourinary tract. J. Am. Soc. Nephrol. **13:**1824–1836.

57. **Sun, Z., A. Amsterdam, G. J. Pazour, D. G. Cole, M. S. Miller, and N. Hopkins.** 2004. A genetic screen in zebrafish identifies cilia genes as a principal cause of cystic kidney. Development **131:**4085–4093.

58. **Takahashi, H., J. P. Calvet, D. Dittemore-Hoover, K. Yoshida, J. J. Grantham, and V. H. Gattone II.** 1991. A hereditary model of slowly progressive polycystic kidney disease in the mouse. J. Am. Soc. Nephrol. **1:**980–989.

59. **Tian, Y., D. Li, J. Dahl, J. You, and T. Benjamin.** 2004. Identification of TAZ as a binding partner of the polyomavirus T antigens. J. Virol. **78:**12657–12664.

60. **Tsiokas, L., E. Kim, T. Arnould, V. P. Sukhatme, and G. Walz.** 1997. Homo- and heterodimeric interactions between the gene products of PKD1 and PKD2. Proc. Natl. Acad. Sci. USA **94:**6965–6970.

61. **Tsvetkov, L. M., K. H. Yeh, S. J. Lee, H. Sun, and H. Zhang.** 1999. p27^{Kip1} ubiquitination and degradation is regulated by the SCF^{Skp2} complex through phosphorylated Thr187 in p27. Curr. Biol. **9:**661–664.

62. **Vassilev, P. M., L. Guo, X. Z. Chen, Y. Segal, J. B. Peng, N. Basora, H. Babakhanlou, G. Cruger, M. Kanazirska, C. Ye, E. M. Brown, M. A. Hediger, and J. Zhou.** 2001. Polycystin-2 is a novel cation channel implicated in defective intracellular Ca^{2+} homeostasis in polycystic kidney disease. Biochem. Biophys. Res. Commun. **282:**341–350.

63. **Winocour, E.** 1963. Purification of polyomavirus. Virology **19:**158–168.

64. **Winston, J. T., P. Strack, P. Beer-Romero, C. Y. Chu, S. J. Elledge, and J. W. Harper.** 1999. The SCFβ-TRCP-ubiquitin ligase complex associates specifically with phosphorylated destruction motifs in IκBα and β-catenin and stimulates IκBα ubiquitination in vitro. Genes Dev. **13:**270–283.

65. **Wu, G., V. D'Agati, Y. Cai, G. Markowitz, J. H. Park, D. M. Reynolds, Y. Maeda, T. C. Le, H. Hou, Jr., R. Kucherlapati, W. Edelmann, and S. Somlo.** 1998. Somatic inactivation of Pkd2 results in polycystic kidney disease. Cell **93:**177–188.

66. **Wu, G., and S. Somlo.** 2000. Molecular genetics and mechanism of autosomal dominant polycystic kidney disease. Mol. Genet. Metab. **69:**1–15.

67. **Yoder, B. K., X. Hou, and L. M. Guay-Woodford.** 2002. The polycystic kidney disease proteins, polycystin-1, polycystin-2, polaris, and cystin, are co-localized in renal cilia. J. Am. Soc. Nephrol. **13:**2508–2516.

68. **Zolotnitskaya, A., and L. M. Satlin.** 1999. Developmental expression of ROMK in rat kidney. Am. J. Physiol. **276:**F825–F836.